Eur J Plant Pathol (2009) 125:159–171
DOI 10.1007/s10658-009-9467-6

Comparison of mycelial proteomes of two *Verticillium albo-atrum* pathotypes from hop

Stanislav Mandelc · Sebastjan Radisek · Polona Jamnik · Branka Javornik

Received: 16 December 2008 / Accepted: 26 March 2009 / Published online: 30 April 2009

Abstract Verticillium wilt diseases caused by *Verticillium* spp. are known in many important crops and can seriously threaten their production. We studied *Verticillium albo-atrum* by comparative analysis of the proteome of four hop isolates, classified by the severity of wilt symptoms as mild and lethal pathotypes, from two geographic origins. A two-dimensional electrophoresis reference map of mycelium proteins was first established, resolving up to 650 protein spots on Coomassie-stained gels in a range of pH 4–7 and M_W 14 – 116 kDa. The average coefficient of variance for the 268 matched protein spots was 16% and 15%, respectively, for technical and biological variability. Principal component analysis (PCA) discriminated the geographic origin of the isolates and between the two pathotypes and showed a closer relationship among English isolates than Slovene ones. The two-dimensional electrophoresis patterns of one mild (PG1) with one lethal pathotype (PG2) from Slovenia and one mild (M) with one lethal pathotype (PV1) from England were compared. A total of 27 and 30 spots were found differentially expressed between the pathotypes, which were analysed by tandem mass spectrometry. Fifty-three proteins were identified, of which 17 matched proteins with annotated functions. The lethal pathotypes showed increased expression of peroxiredoxine and ascorbate peroxidase, a higher level of cytoskeleton components and regulators, and a higher rate of protein synthesis and energy metabolism. These results reveal differences in the expression level of the identified proteins between the two pathotypes and are discussed in relation to virulence.

Keywords Fungi · Proteomic · Two-dimensional electrophoresis · Virulence

Electronic supplementary material The online version of this article (doi:10.1007/s10658-009-9467-6) contains supplementary material, which is available to authorized users.

S. Mandelc · B. Javornik (✉)
Biotechnical Faculty, Agronomy Department,
University of Ljubljana,
Jamnikarjeva 101,
1000 Ljubljana, Slovenia
e-mail: branka.javornik@bf.uni-lj.si

S. Radisek
Slovenian Institute for Hop Research and Brewing,
Cesta Zalskega tabora 2,
3310 Zalec, Slovenia

P. Jamnik
Biotechnical Faculty, Food Science and Technology
Department, University of Ljubljana,
Jamnikarjeva 101,
1000 Ljubljana, Slovenia

Introduction

Vascular wilt diseases caused by the soil-borne fungi *Verticillium albo-atrum* and *V. dahliae* are known in many economically important crops and can seriously threaten their production (Engelhard 1957). These

fungi produce resting structures, which allow them to persist in the soil for many years (Wilhelm 1955). Germination of resting structures in response to root exudates (Mol and Scholte 1995) is followed by direct penetration of the root epidermis at the root tip or wounding site. Once inside the xylem vessels, conidia are produced by budding and are carried upwards with the sap flow until trapped at pit cavities or vessel end-walls (Beckman 1987). Germ tubes must then grow to penetrate into adjacent vessels to continue infection (Heinz et al. 1998).

There is evidence suggesting that *Verticillium* spp. can suppress the host defence response near trapping sites and thus colonise a susceptible plant (Gold and Robb 1995; Lee et al. 1992). However, the molecular and cellular mechanisms that underpin the pathogenicity of *Verticillium* spp. are not well understood (Fradin and Thomma 2006). In studies of *Verticillium* pathogenicity, much attention has been given to the production of cell wall-degrading enzymes and various toxins or elicitors, although their role in pathogenesis has not been fully explained (Fradin and Thomma 2006; Robb 2007). We have studied *V. albo-atrum,* which has caused considerable economic damage to hop (Radisek et al. 2003, 2006). First reports of hop wilt came from England in 1924 (Harris 1927), where mild and lethal (progressive) disease forms were described (Keyworth 1942). Later, one mild (M) and three lethal (PV1, PV2, and PV3) pathotypes of *V. albo-atrum* isolates were identified by virulence testing on different sets of hop cultivars (Sewell and Wilson 1974; Clarkson and Heale 1985). In fluctuating (mild) wilt, plants continue to grow although infected, while in lethal wilt, withering of the plants occurs. In Slovenia, the mild form of hop wilt has appeared sporadically since 1974 but an outbreak of the lethal form was reported in 1997 (Radisek et al. 2003). Field isolates were assigned to pathogenicity groups PG1 (mild) and PG2 (lethal) on the basis of virulence tests and variability among isolates, as revealed by AFLP analysis (Radisek et al. 2003).

Furthermore, a number of mild and lethal *V. albo-atrum* hop isolates from different European regions, together with *V. albo-atrum* and *V. dahliea* isolates from other hosts, were evaluated by AFLP analysis. In the case of *V. albo-atrum* hop isolates, all lethal isolates were genetically different from mild isolates. The mild isolates showed a higher variability than lethal ones and clustered into two groups, irrespective of geographic origin, while lethal Slovene and English isolates each formed separate distinct groups. The obtained data suggested a multiple origin of *V. albo-atrum* hop isolates. Additional comparison of lethal isolates from Slovenia and England by virulence testing confirmed that Slovene PG2 isolates represent a new genotype of the lethal PV1 pathotype (Radisek et al. 2006).

To further characterise differences between *V. albo-atrum* mild and lethal pathotypes we used a proteomic methodology. Although not many proteomic data are available for filamentous fungi, despite their importance and the availability of sequenced genomes (Kim et al. 2007), the utility of proteomics studies has been demonstrated by studies of the mycelia proteome (Ebstrup et al. 2005; Fernandez-Acero et al. 2007; Yajima and Kav 2006), secretome (Yajima and Kav 2006; Paper et al. 2007) and subproteomes (Aisif et al. 2006; Schmitt et al. 2006), with identification and functional analysis of their proteins or differentially expressed proteins as a response to changing conditions or development stages.

The main aims of this study were to produce an initial 2-DE reference map of the *V. albo-atrum* proteome and to analyse major protein differences between the two pathotypes. Our 2-DE analysis visualised over 600 proteins from mycelia protein extracts and comparison of 2-DE proteome images of two mild and lethal isolates revealed differences among them. We report here for the first time complex differences in the protein expression level between the two *V. albo-atrum* pathotypes and the identified proteins from lethal pathotypes (PG2 and PV1), with enhanced expression presumably having functions relating to the suppression of the plant defence, building the cytoskeleton, higher protein synthesis and energy metabolism.

Materials and methods

Fungal material

Four different *V. albo-atrum* hop isolates were obtained from the Slovenian Institute for Hop Research and Brewery Žalec. The PG1 (mild) and PG2 (lethal) isolates designated Zup and Roz were collected in Slovenia, while M (mild) and PV1 (lethal)

isolates, designated 1953 and 1985, came from England and were kindly provided by Dr. Dez Barbara (Warwick HRI). Isolates were grown on prune lactose yeast agar (Talboys 1960), which induces the formation of resting structures and sporulation. Spores were collected from the surface of the agar with a sterile 1 ml tip and transferred to 1 ml of sterile ddH_2O. Spore concentration was determined using a light microscope and Bürker-Türk/Türk counting chamber. The spore suspension was diluted with sterile ddH_2O to a final concentration of 10^5 spores ml^{-1} and 1 ml of diluted suspension was used to inoculate 150 ml of modified general fungal medium (0.2% peptone, 0.2% yeast extract, 2% glucose, 0.1% KNO_3). Fungi were left to grow on a rotary shaker at 20°C and 120 rpm in the dark and the mycelium was harvested after 7 days by filtration. Fungal cultivation was independently repeated four times for each isolate. For growth rate assay, flasks with 20 ml of modified general fungal medium were inoculated with 100 µl of spore suspension and fungi were grown under identical conditions to those mentioned above. Mycelium was collected, dried and weighed daily for 7 days. The experiment was performed in two replications for each isolate.

Protein extraction

Proteins were extracted separately from each individual flask as previously described (Jamnik et al. 2006). Mycelium was washed with 0.9% NaCl and weighed, then ground to a fine powder in liquid nitrogen. Cooled extraction buffer [40 mM Tris-HCl (pH 8), 2% CHAPS, 1% DTT, protease inhibitor cocktail (1 tablet per 10 ml of buffer; Roche)] was added in a ratio of 0.5 ml of buffer per 1 g of mycelium and the mixture was vortexed, incubated on ice briefly, sonicated for 10 s in an ultrasonic bath, then centrifuged at 15,000 *g* and 4°C for 20 min. Supernatant was collected and stored at −80°C until analysis. The protein concentration was measured by the modified Bradford method (Bio-Rad) using BSA as standard.

Two-dimensional electrophoresis and image analysis

Proteins (450 µg) were precipitated using a 2D Clean-Up Kit (GE Healthcare), re-suspended in rehydration buffer (7 M urea, 2 M thiourea, 2% CHAPS, 18 mM DTT, 0.5% IPG buffer pH 4–7, 0.002% bromophenolblue) and applied to 13 cm strips, pH 4–7 (GE Healthcare) by rehydration loading. IEF was performed on an IPGphor 3 unit (GE Healthcare) by employing the standard protocol (500 V for 1 h, gradient to 1000 V for 1 h, gradient to 8000 V for 2.5 h, hold at 8000 V for 40 min), preceded by an additional step (2 h at 100 V) because of the high conductivity of the samples. Following IEF, strips were equilibrated and loaded on vertical 12.5% polyacrylamide gels, sealed with agarose solution and run at 10 mA/gel for 15 min and then at 40 mA/gel on an SE 600 Ruby electrophoresis unit (GE Healthcare) until the bromophenolblue front reached the bottom of the gel. Electrophoresis was repeated three times for each individual extract. After electrophoresis, staining with colloidal Coomassie Brilliant Blue G-250 was performed according to Neuhoff. Briefly, gels were fixed in 40% ethanol, 10% acetic acid for 1.5 h and then washed twice for 15 min in dH_2O and placed in a staining solution for 7 days with constant shaking. The gels were then washed with 1% acetic acid and scanned on ImageScanner III (GE Healthcare).

Images were analysed by Image Master Platinum 2D 6.0 (GE Healthcare) for spot detection, gel matching and interclass analysis. Spots on 2-D images were detected automatically and edited manually on each image using control tools such as 3-D view. Spots were quantified using the % volume criterion (the volume of each spot divided by the total volume of all spots in the gel). Gel matching was performed automatically using one landmark, then matches were checked and corrected manually. After spot detection and matching, triplicate gels of the same sample (technical replicates) were combined in synthetic gels to generate four gels (biological replicates) of each isolate. Technical and biological variation was calculated using normalised spot volumes of spots present on all gels. For technical variation, coefficients of variance (CV) were calculated, first within each group of technical replicates, then average values for individual isolates and finally the overall average. CVs of biological variation were calculated using synthetic gels representing biological replicates. Histograms for the matched spots on the gels were also visually analysed for reproducibility.

Normalised spot volumes were used to compare the different samples. Statistical analysis was performed using Student's t-test ($P \leq 0.05$). Fifty-seven spots displaying at least a 1.5-fold protein expression increase or decrease and three random spots were selected for identification by MS/MS analysis.

Furthermore, spot volume data was subjected to principal component analysis (PCA) using GenStat software (VSN International Ltd). Calculations were made first separately for PG1/PG2 and M/PV1 with two data sets for each pair. The first data set included all matched spots (360 spots for Slovene isolates and 474 spots for English isolates) and the second data set comprised differential spots determined by t-test at $P<0.05$ (209 spots for Slovene isolates and 169 spots for English isolates). Finally, all four isolates were compared using data for 268 spots matched between all 45 gels.

In-gel digestion

Protein spots of interest were excised from replicate gels. Proteins in the gel pieces were digested with trypsin (sequencing grade, modified; Promega) using an Investigator ProGest robotic workstation (Genomic Solutions). Briefly, proteins were reduced with DTT (60°C, 20 min), alkylated with iodoacetamide (25°C, 10 min) and then digested with trypsin (37°C, 8 h). The resulting tryptic peptide extract was dried by rotary evaporation using an SC110 Speedvac (Savant Instruments) and dissolved in 0.1% formic acid for LC-MS/MS analysis.

LC-MS/MS and database searching

Peptide solutions were analysed using an HCTultra PTM Discovery System (Bruker Daltonics) coupled to an UltiMate 3000 LC System (Dionex). Peptides were separated on a Monolithic Capillary Column (200 μm i.d. × 5 cm; Dionex) and eluted with a linear gradient from 97% eluent A (3% acetonitrile in water containing 0.05% formic acid), 3% eluent B (80% acetonitrile in water containing 0.04% formic acid) to 55% eluent A, 45% eluent B for 12 min at a flow rate of 2.5 $\mu l/min^{-1}$.

Peptide fragment mass spectra were acquired in data-dependent AutoMS(2) mode with a scan range of 300–1500 m/z (data were the average of three scans) and up to three precursor ions were selected from the MS scan 100–2200 m/z. Precursors were actively excluded within a 1.0 min window, and all singly-charged ions were excluded.

Peptide peaks were detected and deconvoluted automatically using Data Analysis software (Bruker). Mass lists in the form of Mascot Generic Files were created automatically and used as the input for Mascot MS/MS Ions searches of the NCBInr database using the Matrix Science web server (www.matrixscience.com). Searches were done using the NCBInr database with a taxonomy parameter set to fungi. Allowed missed cleavage sites were set to 1, peptide tolerance to±1.5 Da, MS/MS tolerance to±0.5 Da and peptide charge to 2+and 3+. For spots not identified with the Mascot search engine, Mascot Generic Files were used as input for the PepNovo algorithm (http://bix.ucsd.edu/MassSpec) using the same mass tolerance parameters as above. The top 120 resulting peptide sequences were used as a query for the MS-BLAST algorithm (http://www.dove.embl-heidelberg.de/Blast2/msblast.html).

Results

2-DE and image analysis

Two Slovene (PG1, mild and PG2, lethal) and two English (M, mild and PV1, lethal) *V. albo-atrum* isolates were included in the comparative proteome analysis. Isolates were grown under the same conditions and showed no significant difference in growth rate *in vitro*, and mycelial proteins were extracted by an optimised extraction method (Jamnik et al. 2006). The proteins extracted from the whole mycelia of isolates and separated by 2-DE are shown in Fig. 1. In order to maximise the number of visualised spots, the highest recommended quantity of proteins was loaded (450 μg). The high load had no significant effect on the quality of separation (Fig. 1), since the same horizontal streaking in the acidic area was observed when 100 μg were loaded. The streaking has been attributed to fungal cell wall components forming complexes with proteins (Herbert et al. 2006).

Preliminary analysis in the 3–10 pH range revealed that the number of spots in the basic area was low, so a pH range of 4–7 was used in further experiments. Four biological replicates of each isolate and three technical replicates of each sample were included in the experiment (a total of 48 gels). Three gels (two PG1 and one PG2) were excluded from the analysis, since they were identified as outliers visually and also by factor analysis. The total number of analysed gels was therefore 45. High-molecular weight acidic regions displaying streaking and irreproducible regions around some highly abundant spots were also

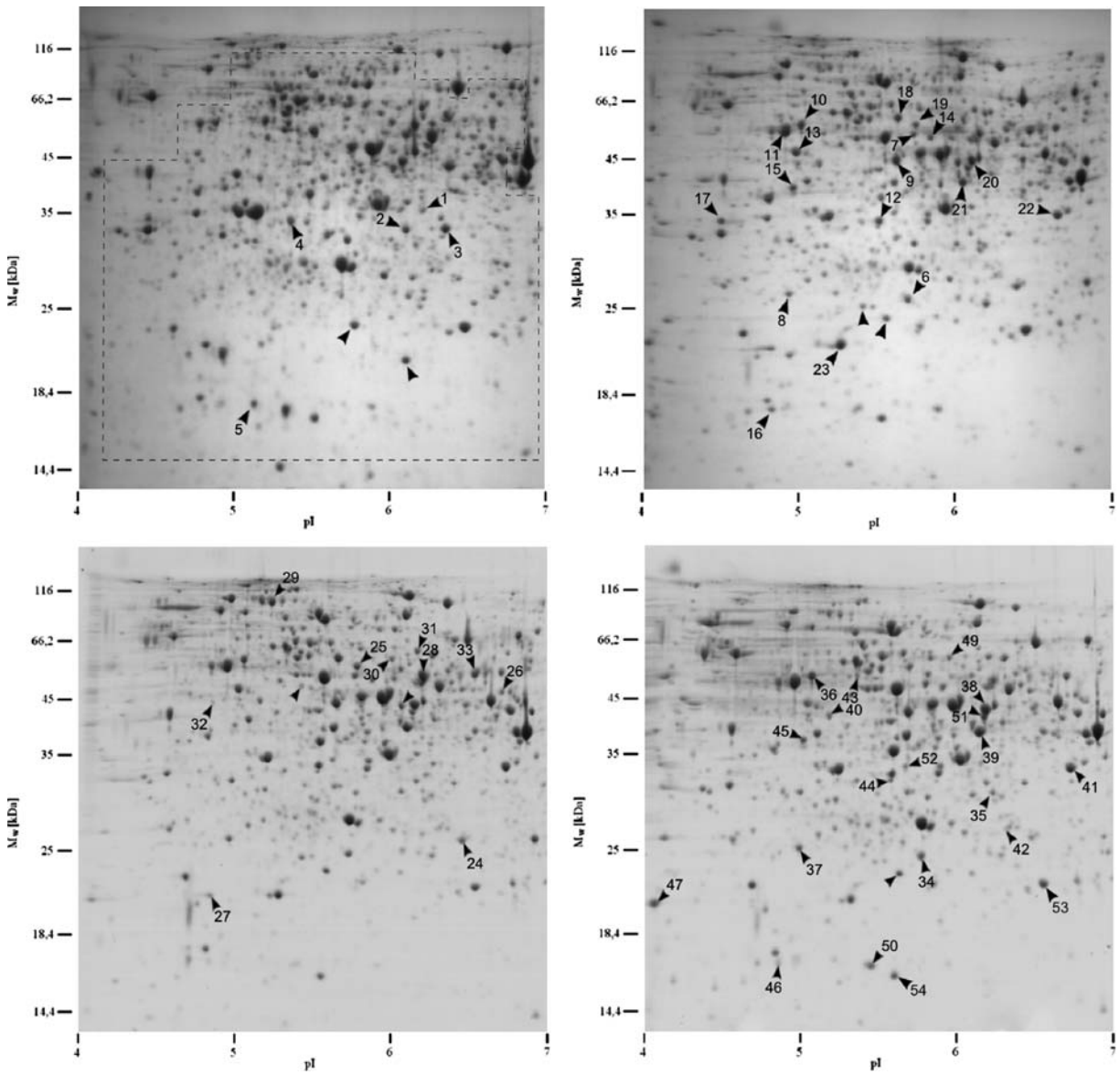

Fig. 1 Representative images of 2-DE PAGE gels of the proteins isolated from the *V. albo-atrum* mild pathotype (upper left PG1, bottom left M) and lethal pathotype (upper right PG2, bottom right PV1); 450 µg of protein was loaded and run on 13 cm IPG strips (pH 4–7). SDS-PAGE (12.5%) was used in the second dimension and the protein spots were visualised by Coomasie Brilliant Blue G-250. Spots analysed by MS/MS are indicated by arrows and identified spots are marked by numbers. Only spots inside the area indicated by dashed lines on the upper left image were used for quantitative analysis

excluded from the analysis (Fig. 2). The number of visualised spots on gels was from 600 to 650 (Fig. 1). The 2-DE patterns of Slovenian and English isolates were highly similar, although with some differences, while there were significant differences in normalised spot volumes.

Data from 268 spots present on all 45 gels were used for estimating technical and biological variation. Coefficients of variance (CV) were calculated within each group of technical replicates, resulting in 87% of CVs <30% (Fig. 3). The average technical CV for individual isolates was 11–24% and an overall average of 16% was achieved. Synthetic gels generated from technical replicates were compared for biological variation calculations and 92% of CVs were <30% (Fig. 3). The average biological CV for

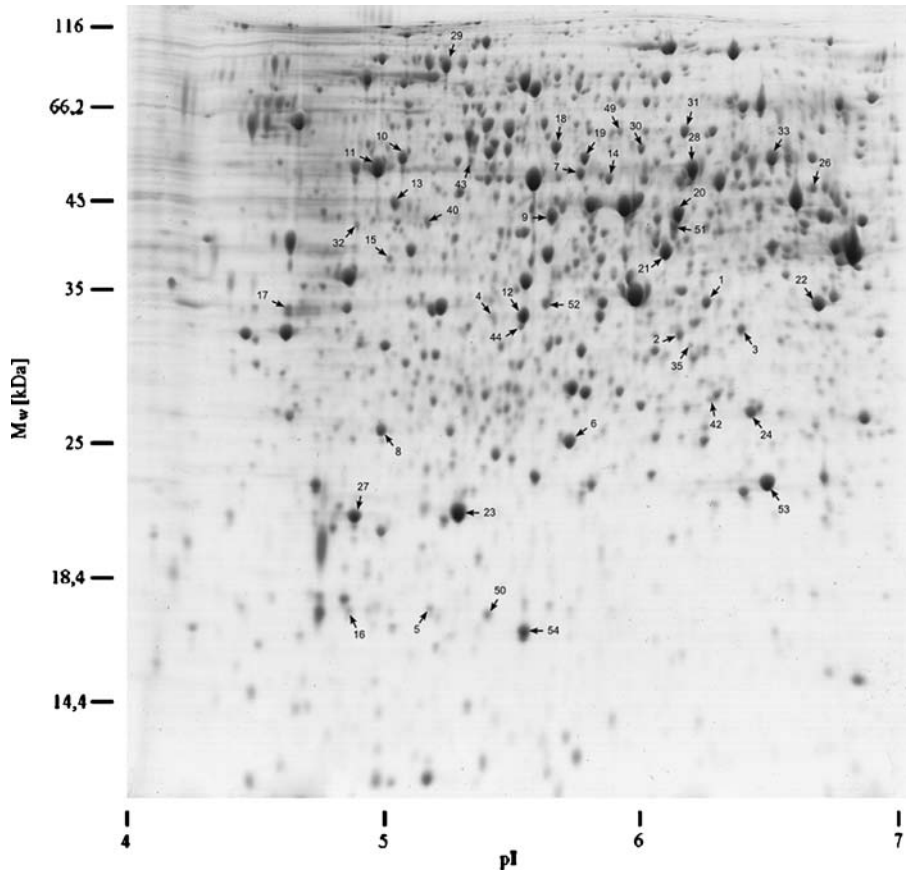

Fig. 2 Reference map of *V. albo-atrum* mycelial proteins. Identified spots are marked with arrows and numbers

individual isolates ranged from 11–21 %, with an overall average of 15%. Biological variation was very low, which was expected considering the clonal nature of *in vitro* fungal cultures.

For differential analysis, spots normalised volume comparison and Student's statistical test were conducted separately for Slovenian and English isolates and spots displaying a significant difference ($P<0.05$) in abundance were considered.

We were able to discriminate the four isolates using PCA. At first, two pathotypes from each geographic location were analysed (Fig. 4a, b). The best separation of isolates was achieved when only differential spots (t-test, $P<0.05$) were used as input data (209 spots for Slovene isolates and 169 spots for English isolates). In the case of Slovene isolates, PC1 explained 76% of variance and discriminated the pathotypes. Samples belonging to lethal isolate PG2 were grouped at large positive values along PC1, while samples of mild isolate PG1 formed two groups at large negative scores on PC1. PC2 explained 7% of variance but it split the PG1 gels into two groups, each containing two biological replications. Such a grouping within an isolate is difficult to explain but is probably linked to unknown factor(s) in cultivation.

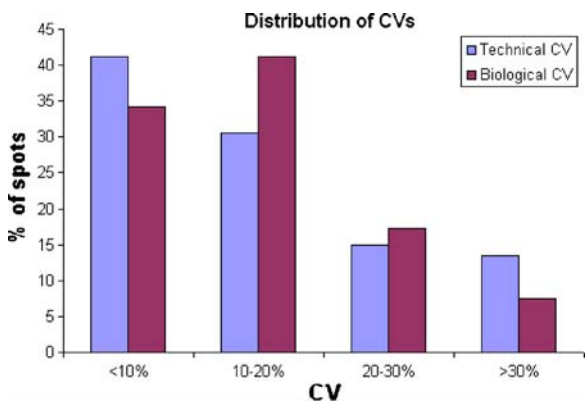

Fig. 3 Distribution of technical and biological coefficients of variance (CV)

Fig. 4 Score plots of PCA analysis. **a** Slovene isolates PG1 and PG2; **b** English isolates M and PV1; **c** Slovene and English isolates PG1, PG2, M and PV1

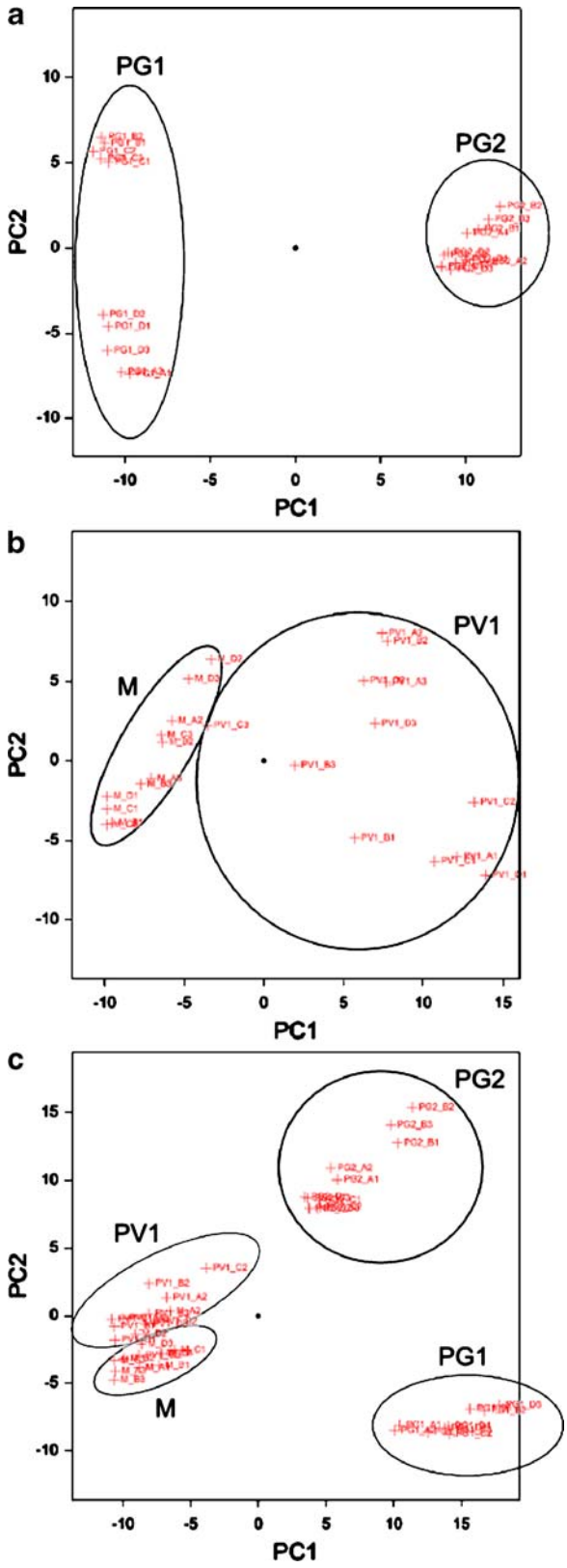

Separation of pathotypes was not so distinct with English isolates, in which PC1 discriminated pathotypes and explained 57% of variation. Finally, all four isolates were compared using spot data of 268 spots, matched between all 45 gels (Fig. 4c). PC1 explained 52% of variation and isolates were discriminated according to geographic origin as Slovene isolates were found at positive scores and English isolates at negative scores on this PC. PC2 explained 13% of variation and discriminated the lethal isolates at positive values from mild isolates at negative values along this PC, whereas Slovene isolates showed more distinct grouping than English ones.

MS/MS analysis

Spots showing a 1.5-fold difference between PG2 and PG1 or PV1 and M isolates together with three random spots were excised from the gels and analysed by LC-MS/MS. A total of 60 spots was chosen, 27 from Slovenian (7 PG1, 20 PG2), 30 from English (10 M, 20 PV1) isolates and three random spots. The resulting spectra were searched against a fungal sequence database (NCBInr) with the Mascot search engine. After discarding protein identifications with only one peptide hit, 53 spots were identified, from which 17 spots were matched to hypothetical proteins with functions predicted on the basis of similarity (supplementary material). Protein identifications, NCBI accession numbers and abundance information are given in Table 1.

We classified the identified proteins into four groups according to function: cytoskeleton components and regulating proteins: beta tubulin (spots 10 and 36), gamma actin (spot 9), Rho3 (spots 8 and 37), GDP dissociation inhibitor (spot 7), and cofilin/actin-depolymerising factor (spot 54); proteins involved in overcoming plant defence: peroxiredoxin (spots 6, 24 and 34), ascorbate peroxidase (spot 35), and manganese superoxide dismutase (spot 53); proteins involved in protein and energy metabolism: ribosomal proteins S2 (spots 15 and 45) and S12 (spots 16 and 46), two DEAD-box RNA helicases (spots 13 and 14), translation initiation factor 5A (spots 27 and 47), elongation factor 2 (spot 1), alpha subunit of NAC (spot 17), proteasome subunit alpha 6 (spot 42), imidazoleglycerol-phosphate synthase (spot 18), O-acetylhomoserine sulfhydrylase (spots 19 and 25), ornithine/acetylornithine aminotransferase (spot 26),

Table 1 Identified proteins, with pI/M_w, MS data and abundance information

Spot no.	Protein Cytoskeleton:	Exp. pI/Mw	Theor. pI/Mw	organism[a]	acc. no.[b]	no. of pept. hits[c]	PG2/PG1 fold diff.[d]	PV1/M fold diff.
10	mix: beta tubulin	5.04/48.8	5.30/48.0	*Verticillium albo-atrum*	ABA61120	25	3.7	1.5
	F0F1 ATP synthase, alpha subunit		9.18/60.4	*Neurospora crassa*	XP_965645	11		
36	beta tubulin	4.96/52.6	5.30/48.0	*Verticillium albo-atrum*	ABA61121	17	3.7	1.5
9	actin, gamma	5.58/42.0	5.54/42.4	*Gibberella zeae*	XP_387511	24	3.9	1.1
8,37	Rho3	4.98/24.8	4.83/23.4	*Saccharomyces cerevisiae*	BAA00897	2	3.5	1.1
7	GDP dissociation inhibitor	5.69/46.8	5.51/51.2	*Neurospora crassa*	XP_962059	8	3.8	1.0
54	cofilin/actin-depolymerising factor	5.51/14.6	5.48/16.7	*Magnaporthe grisea*	XP_360621	2	1.2	−1.1
	ROS degradation:							
6,34	peroxiredoxin (PRX), 1-Cys family	5.67/23.9	5.57/25.1	*Chaetomium globosum*	XP_001226164	5	4.6	1.2
24	peroxiredoxin (PRX), 1-Cys family	6.26/26.5	5.57/25.1	*Chaetomium globosum*	XP_001226164	6	4.2	−1.9
35	ascorbate peroxidase	6.03/31.3	8.87/39.8	*Chaetomium globosum*	XP_001220788	4	3.1	2.0
53	manganese superoxide dismutase	6.38/21.1	6.03/23.0	*Glomerella graminicola*	AAL27457	3	−1.1	−1.6
	Protein and aminoacid metabolism:							
15,45	40 S ribosomal protein S2	4.99/37.7	4.76/31.8	*Gibberella zeae*	XP_391081	6	3.7	2.4
16,46	40 S ribosomal protein S12	4.88/15.1	5.62/14.9	*Gibberella zeae*	XP_387468	13	3.5	1.7
13	translation initiation factor 4F (DEAD-box helicase)	5.01/43.5	5.01/45.0	*Chaetomium globosum*	XP_001220184	20	PG2 only	1.2
14	ATP-dependent RNA helicase (DEAD-box helicase)	5.79/46.3	5.70/49.6	*Magnaporthe grisea*	XP_366730	12	2.5	−1.1
17	NAC alpha subunit	4.56/32.5	4.53/23.1	*Gibberella zeae*	XP_388736	6	2.0	1.3
27	translation initiation factor 5A (eIF-5A)	4.76/22.2	4.78/17.4	*Vanderwaltozyma polyspora*	XP_001644190	4	/	M only
47	translation initiation factor 5A (eIF-5A)	4.05/21.9	4.78/17.4	*Vanderwaltozyma polyspora*	XP_001644190	4	/	2.2
1	elongation factor 2	6.14/33.6	6.03/93.5	*Neurospora crassa*	AAK49353	10	−2.9	−3.9
28	NADP-specific glutamate dehydrogenase	6.03/47.7	6.06/49.2	*Neurospora crassa*	1003201A	8	−1.8	−2.3
18	imidazoleglycerol-phosphate synthase	5.59/49.5	5.83/60.2	*Phaeosphaeria nodorum*	EAT76681	5	8.5	−1.5
19,25	O-acetylhomoserine sulfhydrylase	5.70/48.4	6.06/47.0	*Phaeosphaeria nodorum*	EAT91462	10	2.0	−1.5
26	ornithine/acetylornithine aminotransferase	6.50/44.4	5.90/48.2	*Gibberella zeae*	XP_385722	11	−1.3	−1.8
43	mix: acetylglutamate kinase	5.22/52.3	5.50/58.2	*Gibberella zeae*	XP_388602	3	1.2	1.5
	F0F1 ATP synthase subunit alpha		9.14/60.3	*Aspergillus niger*	XP_001398041	2		
	glycosyl hydrolase family 3		5.35/105.1	*Sclerotinia sclerotiorum*	XP_001593603	2		
	Energy metabolism:							
42	mix: malate dehydrogenase	6.11/27.5	8.80/35.7	*Neurospora crassa,*	XP_958408	13	PG2 only	1.9

	proteasome subunit alpha type 6		5.76/28.0	*Botryotinia fuckeliana*	XP_001548586	9		
20,38	phosphoglycerate kinase	6.04/42.0	5.98/45.2	*Trichoderma viride*	CAA38181	13	6.2	−1.1
4	fructose-1,6-bisphosphate aldolase type IIA	5.38/30.2	5.60/39.8	*Magnaporthe grisea*	XP_369021	7	−2.2	1.1
21,39	fructose-1,6-bisphosphate aldolase type IIA	5.99/38.4	5.53/41.9	*Magnaporthe grisea*	XP_369021	3	5.1	1.2
40	succinyl-CoA synthetase beta subunit	5.06/43.0	5.50/49.3	*Aspergillus clavatus*	XP_001274764	10	−1.1	1.5
22,41	malate dehydrogenase	6.56/33.6	6.47/34.5	*Gibberella zeae*	XP_382680	10	6.3	1.4
12	inorganic pyrophosphatase	5.48/32.3	5.28/32.8	*Neurospora crassa*	Q6MVH7	9	3.6	1.1
44	inorganic pyrophosphatase	5.40/33.3	5.29/32.8	*Magnaporthe grisea*	XP_363672	4	−1.1	2.4
11	mix: F0F1 ATP synthase, beta subunit	4.94/47.4	5.10/55.7	*Neurospora crassa*	XP_963253	21	3.3	1.1
	F0F1 ATP synthase, alpha subunit		9.28/59.6	*Magnaporthe grisea*	XP_367848	6		
32	ATP synthase beta chain, mitochondrial	4.78/42.8	5.23/55.8	*Coccidioides immitis*	*XP_001242378*	12	−2.1	−2.0
	Other:							
2	5'-methylthioadenosine phosphorylase	6.05/31.1	5.99/34.0	*Chaetomium globosum*	XP_001227119	2	−2.3	−1.1
3	predicted esterase	6.27/31.1	6.75/33.0	*Coccidioides immitis*	XP_001245272	2	−3.2	−1.2
5	acetyltransferase (GNAT) family	5.16/13.8	6.31/19.8	*Neurospora crassa*	EAA36297	10	−2.2	1.3
23	similar to *Aspergillus nidulans* CipC protein	5.26/19.9	5.21/15.0	*Phaeosphaeria nodorum*	EAT81580	3	6.3	−1.2
29	alkaline phosphatase	5.13/78.4	5.98/72.2	*Gibberella zeae*	XP_387551	3	1.3	−2.0
30	nitrilotriacetate monooxygenase	5.85/52.8	5.08/60.5	*Gibberella zeae*	XP_391741	2	−1.4	−1.4
33	nitrilotriacetate monooxygenase	6.34/48.6	6.23/53.8	*Aspergillus niger*	XP_001398595	2	2.1	−2.1
31	UDP-galactopyranose mutase	6.00/55.2	5.55/57.1	*Aspergillus oryzae*	BAE60967	6	−1.3	−1.4
49	UDP-galactopyranose mutase	5.77/56.4	5.55/57.1	*Aspergillus oryzae*	BAE60967	7	1.1	1.7
50	probable cyanate lyase	5.28/17.9	5.31/13.9	*Pichia stipitis*	XP_001386400	4	−1.8	4.6
51	S-adenosylmethionine synthetase	5.97/41.1	5.67/43.1	*Neurospora crassa*	XP_965430	8	−1.3	1.5
52	PdxS (subunit of the pyridoxal 5'-phosphate synthase)	5.49/34.6	5.83/33.7	*Magnaporthe grisea*	XP_369484	0032	2.0	1.4

[a] organism with the highest peptide score hit

[b] NCBI accession number

[c] total number of peptides identified from MS/MS spectra

[d] fold difference in protein quantity between mild and lethal pathotype (negative numbers indicate down-regulation)

acetylglutamate kinase (spot 43), NADP-specific glutamate dehydrogenase (spot 28), phosphoglycerate kinase (spots 20 and 38), fructose bisphosphate aldolase type IIA (spots 4, 21 and 39), beta subunit of succinyl-CoA synthetase (spot 40), malate dehydrogenase (spots 22, 41 and 42), inorganic pyrophosphatase (spot 12 and 44), and α- and β- subunits of ATP synthase (spots 10, 11, 32 and 43); other proteins: 5'-methylthioadenosine (MTA) phosphorylase (spot 2), predicted esterase (spot 3), UDP-galactopyranose mutase (spots 31 and 49), acetyltransferase (GNAT) family (spot 5), glycosyl hydrolase family 3 (spot 43), S-adenosylmethionine synthetase (spot 51), protein similar to the CipC protein from *Aspergillus nidulans* (spot 23), alkaline phosphatase (spot 29), nitrilotriacetate monooxygenase (spots 30 and 33), probable cyanate lyase (spot 50), and subunit of pyridoxal 5'-phosphate synthase (spot 52).

Discussion

The aim of this study was to establish a reference 2-D pattern of *V. albo-atrum* proteins and to characterise differences between mild and lethal hop pathotypes using a 2-DE proteomic approach. The pathotypes were grown in nutrient rich culture medium which is favourable and common for growing filamentous fungi but is different from the natural environment. A 2-D reference map of mycelium proteins resolved up to 650 protein spots on CBB stained gels in a range of pH 4–7 and Mw 14 – 116 kDa (Fig. 2). A very high reproducibility of biological and technical replicates within the four analysed isolates was achieved by uniform growth conditions and standard protocols for protein extraction and 2-D PAGE. The average coefficient of variance for the 268 protein spots detected was 16% and 15%, respectively, for technical and biological variability. Such variability is well within reported values (Molloy et al. 2003; Jorge et al. 2005) and indicated that the 2-DE images were acceptable for differential analysis of the isolates. A comparison of 2-DE protein expression patterns was made between Slovene mild and lethal (PG1/PG2) pathotypes and between English mild and lethal (M/PV1) pathotypes. Although the 2-DE patterns of Slovene and English isolates were highly similar, with only minor differences in the presence/absence of spots, there were significant differences in normalised spot volumes, since ~70% of spots displayed differential expression at $P<0.05$ between PG1/M and PG2/PV1. In order to account for these differences among the isolates, PCA was applied, as a multivariant statistical method. PCA clearly separated isolates from Slovenia and England according to geographic origin, as well as their virulence, grouping Slovene isolates further apart than English ones.

These results support the clustering of mild and lethal pathotypes as obtained by DNA analysis (Radisek et al. 2006) and confirmed the variability of the same pathotype from two different geographic locations. However, in the contrast with DNA analysis, the proteomic analysis showed higher relatedness of isolates from the same geographical origin. Comparative analysis was therefore performed between mild and lethal isolates from the same geographic origin, in order to identify differentially expressed proteins in the two pathotypes, since we reasoned that they might display some similarities in their pathogenicity. A total of 60 spots was analysed by LC-MS/MS of which 53 gave more than one peptide hit in the similarity search. The identified proteins were classified according to function into four groups and their putative/presumed role in the mechanism of increased virulence was inferred.

Proteins involved in cytoskeleton assembly and regulation

Four proteins identified in this study are involved in cytoskeleton assembly and regulation. All four were more abundant in the lethal pathotype (beta tubulin in PG2 and PV1; Rho3, gamma actin and GDP dissociation inhibitor in PG2). Tubulin and actin are the main building blocks of microtubules and microfilaments, while the other two proteins are regulatory proteins. Rho GTPases regulate cell polarity and motility by affecting the actin cytoskeletal organisation and are also involved in regulating secretion and clathrin-dependent endocytosis (Ridley 2006). In yeast, Rho3 is necessary for cell growth, and especially for bud growth, which needs cell polarity for directed deposition of new cell wall components (Matsui and Tohe 1992). GDP dissociation inhibitors are regulatory proteins of either Rho GTPases or Rab proteins, which are localised at the cytoplasmic face of organelles and vesicles involved in the biosyn-

thetic, secretory and endocytic pathways in eukaryotic cells (Ueda et al. 1990).

Altogether, an increased level of cytoskeleton components and regulation factors could contribute significantly to the increased virulence of the lethal pathotype, since the cytoskeleton plays an important role in producing the force needed for root penetration, in the spore budding process and in the secretion of cell wall-degrading enzymes, toxins and other virulence factors.

Proteins involved in overcoming plant defence

The xylem parenchyma cells surrounding spore trapping sites deploy an array of defence mechanisms in response to the pathogen. One of the most rapid reactions of a plant following recognition of a pathogen is the production of reactive oxygen species (ROS) (Lamb and Dixon 1997) and pathogens often produce enzymes that degrade ROS. Three peroxide-degrading enzymes were identified in this study, peroxiredoxin, ascorbate peroxidase and manganese superoxide dismutase. Peroxiredoxin from the 1-Cys family was identified from two different spots, indicating different isoform or post-translational modifications. One of them was up-regulated in PG2 and PV1 and the other was up-regulated in PG2 and down-regulated in PV1. Ascorbate peroxidase was found to be up-regulated in PG2 and PV1, while manganese superoxide dismutase was down-regulated in PV1. These peroxide-degrading enzymes might explain a considerable portion of the difference in virulence between the two pathotypes, since faster degradation of ROS could slow down the plant defence response, providing time for the fungus to escape to adjacent vessels.

Proteins involved in protein and energy metabolism

The 40S ribosomal proteins S2 and S12, two DEAD-box RNA helicases (one of them a subunit of translation initiation factor 4F), translation initiation factor 5A, proteasome subunit alpha 6 and an alpha subunit of nascent polypeptide-associated complex (NAC) were found to be up-regulated in PG2 and/or PV1. Ribosomal proteins S2 and S12 are two of 32 proteins in the small ribosomal subunit, while DEAD-box RNA helicases are involved in modulation of the RNA structure and thereby influence processes that include RNA synthesis and modification, ribosome assembly, translation initiation and mRNA stabilisation and degradation (Cordin et al. 2006). Translation initiation factor 5A is involved in peptide bond synthesis. It stimulates efficient translation and peptide-bond synthesis on native or reconstituted 70S ribosomes *in vitro*. It was identified in both M and PV1 gels, but from different spots, indicating different post-translational modifications. The alpha subunit of NAC is a multifunctional eukaryotic protein involved in translation and subcellular targeting of nascent polypeptides, but it has also been shown to function as a transcription coactivator (Rospert et al. 2002). NADP-specific glutamate dehydrogenase, which catalyses conversion of glutamate to α-ketoglutarate and ammonia, was down-regulated in PG2 and PV1. Some enzymes from aminoacid biosynthesis pathways were also identified: imidazoleglycerol-phosphate synthase (histidine biosynthesis) was up-regulated in PG2, O-acetylhomoserine sulfhydrylase (methionine biosynthesis) was up-regulated in PG2 but down-regulated in PV1, ornithine/acetylornithine aminotransferase (arginine biosynthesis) was down-regulated in PV1 and acetylglutamate kinase (arginine biosynthesis) was up-regulated in PV1. On the other hand, an increased amount of elongation factor 2 was detected in PG1, although the discrepancy between theoretical Mw (93 kDa) and experimental Mw (34 kDa) and the accumulation of peptide hits in one part of the amino acid sequence indicates its proteolytic degradation.

These results indicate that the lethal pathotype might be more active in terms of protein synthesis and protein secretion (increased level of NAC) than the mild pathotype. Since protein synthesis is an energy-consuming process, higher levels of the carbohydrate metabolism enzymes phosphoglycerate kinase, fructose bisphosphate aldolase type IIA, beta subunit of succinyl-CoA synthetase and malate dehydrogenase are not surprising. Malate dehydrogenase was also considered to be a pathogenicity factor in *Botrytis cinerea* (Fernandez-Acero et al. 2006) since it catalyses the conversion of malate to oxaloacetate, which is a substrate for oxalic acid synthesis. Secretion of oxalic acid creates an acidic environment, triggering expression and secretion of virulence factors and phytotoxins. Inorganic pyrophosphatase, α- and β- subunits of ATP synthase, were also present in higher levels, confirming increased energy production and consumption in PG2 and PV1.

Other identified proteins

PG1 showed a higher abundance of 5'-methylthioadenosine (MTA) phosphorylase, which catalyses the recycling of MTA, a side-product of polyamine synthesis. Polyamines have numerous functions in all living organisms and are necessary for cell growth, development and division. They have been shown to have a role in plant-pathogen interactions, since intercellular levels of free and conjugated polyamines are often increased after infection (Walters 2003). Polyamines serve as a substrate for cell-wall localised oxidases, yielding H_2O_2.

UDP- galactopyranose mutase is involved in the conversion of UDP-D-galactopyranose into UDP-D-galacto-1,4-furanose through a 2-keto intermediate. This reaction is part of a pathway of cell wall component synthesis, so different forms of this enzyme in M and PV1 might lead to different cell wall compositions, affecting the plant's ability to recognise the pathogen.

S-adenosylmethionine synthetase catalyses the formation of S-adenosyl-L-methionine (SAM) from methionine and ATP. SAM is involved in numerous methyl-transfer reactions and is also a substrate for the synthesis of ethylene in plants.

GNAT family of acetyltransferases is one of the five families of histone acetyltransferases with members having important roles in cell growth and development.

Conclusion

In conclusion, we investigated proteome-level differences between two *V. albo-atrum* pathotypes from hop using two-dimensional electrophoresis and mass spectrometry. To our knowledge, this is the first report of *V. albo-atrum* protein identification using a proteomic approach. It describes the protein profiles of two hop pathotypes of *V. albo-atrum* and it provides 53 identified proteins that indicate complex differences at the protein expression level. The 2D-protein map established in this study will serve as a basis and reference source for future proteome analysis, and the identified proteins can help with validation of genome annotation and functional analysis of the virulence mechanism in recently released or in the next release of genome sequences of plant pathogenic *Verticillium* species.

Acknowledgements This study was funded by the Ministry of Higher Education, Science and Technology; contracts no. L4-7179, P4-0077 and S4-486-116/1000-05-310050. The authors thank Dr. Rajcevic Uros from NorLux Neuro-Oncology/Crp Sante, Luxembourg, for help in interpreting MS/MS data. We are grateful to Dr. Jesus Jorrin from the Department of Biochemistry and Molecular Biology, University of Cordoba, Cordoba, Spain, for critical reading of the manuscript and for thoughtful suggestions.

References

Aisif, A. R., Oellerich, M., Amstrong, V. W., Riemenschneider, B., Monod, M., & Reichard, U. (2006). Proteome of conidial surface associated proteins of *Aspergillus fumigatus* reflecting potential vaccine candidates and allergens. *Journal of Proteome Research, 5*, 954–962. doi:10.1021/pr0504586.

Beckman, C. H. (1987). *The nature of wilt disease in plants*. St Paul, MN: The American Phytopathological Society.

Clarkson, J. M., & Heale, J. B. (1985). Pathogenicity and colonization studies on wild-type and auxotrophic isolates of *Verticillium albo-atrum* from hop. *Plant Pathology, 34*, 119–128. doi:10.1111/j.1365-3059.1985.tb02768.x.

Cordin, O., Banroques, J., Tanner, N. K., & Linder, P. (2006). The DEAD-box protein family of RNA helicases. *Gene, 367*, 17–37. doi:10.1016/j.gene.2005.10.019.

Ebstrup, T., Saalbach, G., & Egsgaard, H. (2005). A proteomics study of in vitro cyst germination and appressoria formation in *Phytophthora infestans*. *Proteomics, 5*, 2839–2848. doi:10.1002/pmic.200401173.

Engelhard, A. W. (1957) Host index of *Verticillium albo-atrum* Reinke and Berth, (including *Verticillium dahliae* Kleb.). In: *Supplement to Plant Disease Reporter No. 244*, pp. 23-49.

Fernandez-Acero, F. J., Jorge, I., Calvo, E., Vallejo, I., Carbu, M., Camafeita, E., et al. (2006). Two-dimensional electrophoresis protein profile of the phytopathogenic fungus *Botrytis cinerea*. *Proteomics, 6*, S88–S96. doi:10.1002/pmic.200500436.

Fernandez-Acero, F. J., Jorge, I., Calvo, E., Vallejo, I., Carbu, M., Camafeita, E., et al. (2007). Proteomic analysis of phytopathogenic fungus *Botrytis cinerea* as a potential tool for identifying pathogenicity factors, therapeutic targets and for basic research. *Archives of Microbiology, 187*, 207–215. doi:10.1007/s00203-006-0188-3.

Fradin, E. F., & Thomma, B. (2006). Physiology and molecular aspects of Verticillium wilt diseases caused by *V. dahliae* and *V. albo-atrum*. *Molecular Plant Pathology, 7*, 71–86. doi:10.1111/j.1364-3703.2006.00323.x.

Gold, J., & Robb, J. (1995). The role of the coating response in Craigella tomatoes infected with *Verticillium dahliae*, race-1 and race-2. *Physiological and Molecular Plant Pathology, 47*, 141–157. doi:10.1006/pmpp.1995.1048.

Harris, R. V. (1927). A wilt disease of hops. In: *East Malling Research Station Annual Report for 1925, Supplement II.* pp. 92–93.

Heinz, R., Lee, S. W., Saparno, A., Nazar, R. N., & Robb, J. (1998). Cyclical systemic colonization in *Verticillium*-infected tomato. *Physiological and Molecular Plant Pathology, 52*, 385–396. doi:10.1006/pmpp.1998.0163.

Herbert, B. R., Grinyer, J., McCarthy, J. T., Isaacs, M., Harry, E. J., Nevalainen, H., et al. (2006). Improved 2-DE of microorganisms after acidic extraction. *Electrophoresis, 27*, 1630–1640. doi:10.1002/elps.200500753.

Jamnik, P., Radisek, S., Javornik, B., & Raspor, P. (2006). 2-D Separation of *Verticillium albo-atrum* proteins. *Acta Agriculturae Slovenica, 87*, 455–460.

Jorge, I., Navarro, R. M., Lenz, D., Ariza, D., Porras, C., & Jorrin, J. (2005). The Holm Oak leaf proteome: Analytical and biological variability in the protein expression level assessed by 2-DE and protein identification tandem mass spectrometry *de novo* sequencing and sequence similarity search. *Proteomics, 5*, 222–234. doi:10.1002/pmic.200400893.

Keyworth, W. G. (1942). Verticillium wilt of the hop (*Humulus lupulus*). *The Annals of Applied Biology, 29*, 346–357. doi:10.1111/j.1744-7348.1942.tb06138.x.

Kim, Y., Nandakumar, M. P., & Marten, M. R. (2007). Proteomics of filamentous fungi. *Trends in Biotechnology, 25*, 395–400. doi:10.1016/j.tibtech.2007.07.008.

Lamb, C., & Dixon, R. A. (1997). The oxidative burst in plant disease resistance. *Annual Review of Plant Physiology, 48*, 251–275. doi:10.1146/annurev.arplant.48.1.251.

Lee, S. W., Mazar, R. N., Powell, D. A., & Robb, J. (1992). Reduced PAL gene expression in *Verticillium*-infected resistant tomato. *Plant Molecular Biology, 18*, 345–352. doi:10.1007/BF00034961.

Matsui, Y., & Tohe, A. (1992). Yeast *Rho3* and *Rho4 RAS* superfamily genes are necessary for bud growth, and their defect is suppressed by a high-dose of bud formation genes *cdc42* and *bem1*. *Molecular and Cellular Biology, 12*, 5690–5699.

Mol, L., & Scholte, K. (1995). Formation of microsclerotia of *Verticillium dahliae* Kleb on various plant-parts of two potato cultivars. *Potato Research, 38*, 143–150. doi:10.1007/BF02357927.

Molloy, M. P., Brzezinski, E. E., Hang, J., McDowell, M. T., & VanBogelen, R. A. (2003). Overcoming technical and biological variation in quantitative proteomics. *Proteomics, 3*, 1912–1919. doi:10.1002/pmic.200300534.

Paper, J. M., Scott-Craig, J. S., Adhikari, N. D., Cuom, C. A., & Walton, J. D. (2007). Comparative proteomics of extracellular proteins in vitro and in planta from the pathogenic fungus *Fusarium graminearum*. *Proteomics, 7*, 3171–3183. doi:10.1002/pmic.200700184.

Radisek, S., Jakse, J., Simoncic, A., & Javornik, B. (2003). Characterization of *Verticillium albo-atrum* field isolates using pathogenicity data and AFLP analysis. *Plant Disease, 87*, 633–638. doi:10.1094/PDIS.2003.87.6.633.

Radisek, S., Jakse, J., & Javornik, B. (2006). Genetic variability and virulence among *Verticillium albo-atrum* isolates from hop. *European Journal of Plant Pathology, 116*, 301–314. doi:10.1007/s10658-006-9061-0.

Ridley, A. J. (2006). Rho GTPases and actin dynamics in membrane protrusions and vesicle trafficking. *Trends in Cell Biology, 16*, 522–529. doi:10.1016/j.tcb.2006.08.006.

Robb, J. (2007). *Verticillium* tolerance: resistance, susceptibility, or mutualism? *Canadian Journal of Botany, 85*, 903–910. doi:10.1139/B07-093.

Rospert, S., Dubaquie, Y., & Gautschi, M. (2002). Nascent-polypeptide-associated complex. *Cellular and Molecular Life Sciences, 59*, 1632–1639. doi:10.1007/PL00012490.

Schmitt, S., Prokisch, H., Schlunck, T., Camp, D. G., Ahting, U., Waizenegger, T., et al. (2006). Proteome analysis of mitochondrial outer membrane from *Neurospora crassa*. *Proteomics, 6*, 72–80. doi:10.1002/pmic.200402084.

Sewell, G. W. F., & Wilson, J. F. (1974). Hop wilt, soil temperature and nitrogen. In: *East Malling Research Station Annual Report for1973*. pp. 203–204.

Talboys, P. W. (1960). A culture-medium aiding the identification of *Verticillium albo-atrum* and *V. dahliae*. *Plant Pathology, 9*, 57–58. doi:10.1111/j.1365-3059.1960.tb01147.x.

Ueda, T., Kikuchi, A., Ohga, N., Yamamoto, J., & Takai, Y. (1990). Purification and characterization from bovine brain cytosol of a novel regulatory protein inhibiting/ the dissociation of GDP from and the subsequent binding of GTP to RhoB p20, a RAS p21-like GTP-binding protein. *Journal of Biological Chemistry, 265*, 9373–9380.

Walters, D. (2003). Resistance to plant pathogens: possible roles for free polyamines and polyamine catabolism. *New Phytologist, 159*, 109–115. doi:10.1046/j.1469-8137.2003.00802.x.

Wilhelm, S. (1955). Longevity of the Verticillium wilt fungus in the laboratory and in the field. *Phytopathology, 45*, 180–181.

Yajima, W., & Kav, N. N. V. (2006). The proteome of the phytopathogenic fungus *Sclerotinia sclerotiorum*. *Proteomics, 6*, 5995–6007. doi:10.1002/pmic.200600424.